Analysis of 3-D P-S seismic data: Joffre, Alberta

Glenn A. Larson and Robert R. Stewart

ABSTRACT

A 3-D P-S seismic survey acquired in the Joffre region of central Alberta has provided a cost-effective manner to acquire shear data volumes. The data discussed here were acquired by the Colorado School of Mines (Al-Bastaki et al., 1994) and processed by Pulsonic Geophysical Ltd. Three one square mile data sets are further analyzed in this paper: The conventional pure P-wave data and two anisotropic converted-wave products (the P-S1 and the P-S2). The shear data are of good quality and allow the construction of Vp/Vs and delay-time maps for both the slow and fast shear-wave polarization. The delay-time maps reveal a localized stress regime that can be mapped at depth. The Vp/Vs maps show an anomaly in the Viking interval which suggests a higher percentage of sand. There is more than one factor affecting the Vp/Vs calculations for the Nisku level, which has prevented making a direct inference of a change of lithology between dolomite and anhydrite.

INTRODUCTION

Three-dimensional (3-D) seismic acquisition is becoming an essential tool in seismic exploration and development. Exploration companies have turned to the 3-D method to optimize investment and minimize risk reduction (Buchanan, 1992). The 3-D seismic survey is a recent development in seismic history. The first 3-D survey was conducted by Exxon in the early 1970's (Robertson, 1992). Production land 3-D surveys were initiated over an oil field in New Mexico in 1973 by a six company consortium, while marine 3-D surveys began in the Gulf of Mexico in 1975. Since then, the number of 3-D surveys acquired worldwide have rapidly increased each year (Oosterbaan, 1990); and presently they are an established practice in exploration and development.

Shear-wave acquisition also has had a long history (Tatham and Stewart, 1993), although its usefulness has not been as quickly exploited as conventional P-wave acquisition. Converted-wave surveys in 2-D have been acquired to infer lithology using Vp/Vs ratios (Garrota and Marechal, 1987; Harrison, 1992). Ensley (1984) use shear-waves in the identification of gas-bearing clastic reservoirs. Shear source 3-D surveys have been acquired and interpreted (Davis et al., 1992), and Al-Bastaki et al. (1994) use the shear source version of the Joffre 3-D multicomponent survey as part of an integrated characterization of the Joffre Nisku reservoir. An extension of converted-wave surveys is to combine 2-D P-SV with a conventional 3-D seismic to construct a multicomponent 3-D survey to provide a more detailed description of the rock volume.

The benefit of recording P-SV data is in acquiring additional elastic wave information at an incremental cost over a conventional (P-P) survey. Only a P-wave source is required with three-component geophones. For a 3-D P-SV survey, Vp/Vs ratios can be mapped over a survey area, providing a wealth of information. The

orientation of the fast shear-wave polarization (S1) and the slow shear-wave polarization (S2) can be determined in processing. It is thought that an identifiable seismic orientation will result from a consistent stress or fracture orientation throughout the sedimentary column. The two shear polarizations can be processed separately, tripling the amount of interpretable data. The variations of the S1 and S2 isochrons between horizons can be mapped as well. Their amplitudes have been used in anisotropic studies and fracture detection (Yardley et al., 1991). For instance, Mueller (1991) found that dimming of the S2 amplitude on 2-D multicomponent lines covering the Austin Chalk in Texas can be used to infer areas of faulting within the reservoir. This data set provides a unique opportunity to apply, for the first time, the established techniques of elastic wave interpretation in 2-D to the third dimension.

We will present interpretative techniques for the 3-D P-SV data set that describe three geologic scenarios: A diagenetic change between a dolomite and anhydrite in the Nisku formation, the estimation of the presence of sand in the Viking formation, and the detection of fractures within the Second White Speckled Shale.

GEOLOGIC BACKGROUND

The Nisku is a carbonate shelf platform within the Upper Devonian (Watts, 1987). The Nisku forms the base of the Winterburn basin of the Western Canada Sedimentary Basin. The Joffre D2 Pool, as deemed by the Energy Resources Conservation Board of Alberta (ERCB), is classified as a light to medium crude oil pool. It is located between Townships 38 and 40, Ranges 26 and 27W4. It was discovered in 1956 at a depth of 2134m. Cumulative production as of 1992 is 7450.2 x 10^3 m^3, with an estimated 2700 x 10^3 m^3 established reserves remaining (ERCB, 1992).

A stratigraphic chart of the Upper Devonian is shown in Figure 1. Various authors (Anderson and Machel, 1987; Stokes, 1987; Machel, 1983; and Chevron Exploration Staff, 1979) have written extensively upon the prolific Zeta Lake pinnacle reefs of the Winterburn basin, however, the literature on the Inner and Outer Shelf to the south east is limited. We will be concentrating upon the Inner Shelf, where the Joffre Field resides. The Joffre field and related pools are centered about the Bashaw complex of the Leduc in central Alberta (Figure 2).

The Leduc topography has provided the relief for the Winterburn carbonates to initiate in this area (Gilhooly, 1986). Other related pools in the area are Stettler, Fenn-Big Valley, Malmo, and Duhammel. These fields involve structural drape over the Leduc. Joffre is a progradational shelf whose trapping mechanism is solely stratigraphic (Rennie et al., 1989).

The Nisku Joffre field is unique because of the nature of its stratigraphic trap. The pool has a diagenetic up dip trap of anhydrite. The Nisku pool is defined by a halo of dolomitized vuggy porosity that has not been plugged by the later-stage anhydrite diagenetic event. Figure 3 displays a Nisku structure map of the Joffre pool and the limit of porosity, as defined by well control. The late-stage anhydrite event also filled in some of the primary porosity of the earlier dolomitization, resulting in reservoir heterogeneity. Conventional P-wave seismic has not been successful in contrasting the dolomite reservoir from the anhydrite because of similar acoustic impedances.

The Viking formation consists of marine-deposited sand and shale sequences that formed a clastic wedge east of the rising Cordillera during Cretaceous time (Reinson et al., 1994). The Viking is a member of the Colorado Group and lies above the Joli Fou shale. It is a prolific producer of oil and gas with the basin. In the Joffre region, sand thicknesses vary between 15 and 35 metres at a depth of about 1500 metres. A producing Viking oil pool which has produced $5822 \times 10 m^3$ of oil, lies 2 miles southwest of the Joffre 3-D P-SV survey.

The Second White Speckled Shale is basin-wide marker on log and seismic data. The shale was formed at the end of a massive sea level rise in the Cretaceous and has a high organic content (Leckie et al, 1994). It is both a source and reservoir of hydrocarbons. Oil has been produced in the shale within zones of intense vertical fracturing brought about by the in situ stress field of the Rocky Mountains. The fracture presence is the key criterion for economic production. The detection of vertical fractures and the measurement of transverse isotropy (due to the finely layered shales) have been investigated by Goodaway and Mayo (1994), and Stewart et al., (1993). The Second White Speckled Shale resides about 1400m below the Joffre survey. There is no production of oil within the shale in the Joffre area.

ACQUISITION AND PROCESSING

The parameters of the survey are detailed in Table 1. The multicomponent survey was acquired over a 13.6 km^2 grid in April of 1993 by the Colorado School of Mines (Al-Bastaki et al., 1994) and Solid State Geophysical Ltd. Acquisition comprised of 4 live receiver patches consisting of 6 lines each. Each patch contained 324 3-component receivers giving a channel demand of 972. The source was a single vibrator that used a 12-second linear up-sweep, repeated 7 times, between 10 and 120 Hertz. The receivers were 3-component OYO SMC-3-D geophones. No surface arrays were used to attenuate ground roll or the air blast.

The source line orientation was at a 45 degree angle to the receiver lines (Figure 4). The survey was designed to smooth out the fold, azimuth, and offset distribution for pure P and pure S waves constrained by a reduced channel capability brought out by a limited availability of three component receivers. This resulted in acquiring with smaller patches of live receivers.

Figure 5 shows the CMP fold map. The fold is well distributed in the east-west direction. The nominal fold is 15 with a maximum fold of 48. Complications result in the common-conversion point (CCP) domain for P-SV ray paths (Eaton and Lawton, 1992). Designing a converted-wave survey becomes complicated because the ray paths between source and receiver are not symmetrical . Designs that do not incorporate the positional variance of the CCP bin can have unpredictable fold patterns. Short wavelength fold variations and fold gaps are detrimental to robust post-stack and pre-stack amplitude mapping (Lawton, 1993).

Gaps in CCP fold distribution will occur if CCP binning is not taken into account in the acquisition design. The Joffre survey was not designed for converted-waves. The converted-wave optimized asymptotic bin map at Vp/Vs = 2 is shown in Figure 6. There are two linear gaps of zero fold coupled with highly periodic fold variation in the east-west direction. These gaps complicate the processing and interpretation of the converted-wave data.

The data were processed by Pulsonic Geophysical Ltd. of Calgary. The flows for the P and the converted-wave data sets are shown in Figures 7 and 8, respectively. The conventional survey was processed with standard 3-D processes that will not be discussed here. The details of the converted-wave processing can be found in Cary (1994). The data were recorded in the inline and crossline components in the field. The data were combined and rotated in the manner described by Lane (1993). Another rotation, based upon the cross-correlation modelling of Harrison (1992), separates the data into slow and past polarizations, S2 and S1 into the natural coordinate system. The azimuth of the natural coordinate system was found to be 45 degrees east of north. Each volume was then separately processed. The key point in the processing was in the smoothing of the CCP fold into the gaps in an attempt to even out the periodicity of the fold, details of which can be found in Cary (_this volume_). The volumes were asymptotically binned at Vp/Vs ratio of 2.

INTERPRETIVE TECHNIQUES

Acquiring and processing a multicomponent 3-D data set results in three data volumes - the conventional P-P, the P-S1, and the P-S2. The conventional P-wave 3-D provides spatial delineation of events whereas the shear sections can give lithologic and bulk rock fabric information.

The interpretative techniques developed here use the migrated products provided by Pulsonic Geophysical Ltd. of Calgary. Each data set consists of 141 inlines and 107 crosslines at a 30m bin spacing. Two seconds (at 2ms sample rate) of the P-wave data and 3.5 seconds (at 4ms sample rate) of the S1 and S2 data were loaded onto the Landmark interpretation system. The inline and crossline geometry is shown in Figure 9. A one square mile patch surrounding the 11-22-39-26W4 well is analyzed.

Figure 10 displays the correlation of the P and P-S1 sections along Crossline 67 of the P-P and P-SV synthetic seismograms. The scale of the P-wave section and P-P synthetic was expanded by 1.5 to facilitate the correlation to the P-S1 section. A tie between Crossline 70 and Inline 40 of the S1 and S2, respectively (Figure 11), shows the mistie between S1 and S2. A mistie of this nature has been documented by Mueller (1991) in sediments above the Austin Chalk in Texas. It is indicative of shear-wave splitting due to the same stress field throughout the sedimentary column.

In Figure 11, the S1 is superior to the S2. S1 provides better continuity of events with higher amplitude and allows easier interpretation. Both shear volumes, however, do have excellent resolution, albeit reduced, in comparison to the P-volume. The reduced resolution in the shear section has not resolved the top of the Mannville peak or the Banff trough, but the other reflectors above the Wabamun are adequately imaged. The units below the Wabamun are not imaged very well, in the P-P and shear volumes, because the Mannville coal in the Cretaceous section has attenuated the reflection energy below it. The attenuation of the reflectors below the Mannville coal is confirmed in the zero-offset VSP of 11-22-39-26W4 (Sun et al., _this volume_). The converted wave sections have, however, managed to image to the Precambrian level.

The amplitudes of the S1 amplitudes in the Crossline display of Figure 11 vary periodically along it, giving the section a mottled appearance. Figure 12 displays in map view the amplitude of an S1 event below the Second White Specks. The amplitudes are periodic in the crossline direction and mimic the fold periodicity in of the acquisition (Figure 6), clearly showing that the amplitudes of the converted shear

volumes have been compromised by the survey design. This has prevented any detailed shear amplitude analysis.

One of the key interpretive tools is the calculation of the ratio between the velocity of the P-wave versus the velocity of the S-wave (the Vp/Vs ratio). By picking time events, we can find low-resolution but robust lithology indicators. Both the conventional and converted-wave sections equally respond to structural changes in the subsurface. Apparent time interval differences between the P, S1 and S2 can be related to changes in the bulk properties of the rocks within the interval. If the variables of the bulk properties can be constrained, then we can make lithologic, porosity, or fracture density inferences. Sensitivities of Vp/Vs ratios to gas saturation, lithology, porosity, and fracturing within a time interval are exploited in this technique. By using other sources of information, changes in the Vp/Vs ratio may be limited to one variable, and inferences upon its variation can be made. For converted waves, the Vp/Vs ratio can be calculated from stacked data sets of P-P and P-S in the following equation:

1) $$\mathbf{Vp/Vs = 2*(Is/Ip) - 1}$$

,where Is= time interval between two P-S reflections

Ip = time interval between two P-P reflections

(Harrison, 1992)

For 3-D data, we can calculate two ratios: Vp/Vs1 and Vp/Vs2. A time slice of the S2 volume and the P-wave volume (Figure 13) shows that the converted-shear and the acoustic data respond to the same structures, in this case, drape of the Banff and Mannville coal over the Leduc pinnacle in the centre of the survey and the Leduc shelf complex in the south east. The ratios calculated between key events can be mapped in plan view and can be related to changes within the intervals of rock fabric, lithology, porosity, clay content, and /or fluid content. Patterns of Vp/Vs ratios can now be mapped. The calculation of the Vp/Vs ratio is a simple by-product of interpreting the P-P and the converted-wave volumes together.

The Vp/Vs ratio also identifies miscorrelations between data volumes while interpreting. Vp/Vs ratios can be easily calculated on the Landmark workstation during the interpretation, and incorrect picks can be found quickly by keeping the ratio within a geologically reasonable value. The time difference or delay between the S1 and S2 for individual horizons are calculated and mapped to infer stress field patterns within the strata.

RESULTS

Figures 14 to 18 display time-delay maps of selected time structure horizons between S1 and S2 from the Cretaceous to the Devonian. The time delay increases with time until the Wabamun level, where there is a slight decrease. At the Nisku level, the delay-time pattern has changed. This may indicate a continuous stress regime from the surface to the base of the Mesozoic. Also, a consistent pattern of time delay overprints each map, inferring a local stress pattern within the Mesozoic.

Figure 19 and 20 display Vp/Vs1 and Vp/Vs2 ratio maps for the Viking formation calculated from two different intervals. The narrower interval, between the

Base of Fish Scales and Mannville, reveal a distinct region of lower Vp/Vs ratio for both S1 and S2. This could be indicative of higher sand content within the Viking interval. The pattern of a lower Vp/Vs anomaly is seen again for the wider interval within Figures 19 and 20 (between the Base of Fish Scales and a marker in the Colorado Group). The anomaly is now more diffuse and the Vp/Vs values are weighted toward sand values because more sand section is included in the calculation. The redundancy of measurement confirms the robustness of the anomaly.

Figure 21 and 22 display the Vp/Vs ratio maps of the Nisku calculated between two different intervals. Both intervals are wide and include most of the Wabamun section. A Vp/Vs ratio of 1.8 for dolomite is expected, however, the values trend toward 2.0 or more which is too high for dolomite.

DISCUSSION

It is crucial, if 3-D multicomponent surveys are to be acquired in the future, that the CCP fold patterns be included in the 3-D design optimization. Lawton(1993) has provided guidelines to optimize the CCP fold distribution. In the field, a high channel demand will be imposed by the 3-component geophones. Logistically, the geophones will have to be laid-out and balanced with greater care than they have done in the past. This will result in longer receiver layout times and higher costs. The costs are mitigated, however, by the return in acquiring 3 data volumes with a conventional P-wave source. Survey design is currently being compromised by a limited number of 3-component geophones in the industry, resulting in small live group patches and narrow azimuths. As the interest in 3-C 3-D work continues, the market will respond to this demand, and more 3-C geophones will become available to allow more flexibility in acquisition design.

Areas of high time delay in Figure 14 to 18 may indicate zones of greater horizontal stress differential in the subsurface within the natural coordinate frame. The 45 degree rotation angle compares favourably with the results of Babcock (1978) who measured well bore break-outs in wells within the basin. For brittle formations, such as the Second White Speckled Shale and the Mannville coal, it is possible that vertical fractures may preferentially occur in these zones. It is unfortunate that the amplitudes of the shear sections were compromised because of inadequate survey design. Mueller (1991) has shown that amplitude changes in S2 (the polarization perpendicular to the cracks) are more sensitive to fracture-induced anisotropy than are time intervals.

The delay-time maps indicate that there is a different stress field orientation in the Paleozoic than there is in the Mesozoic and the near surface. This is probably due to the transition in bulk rock properties from a predominately clastic interval in the Mesozoic to carbonates in the Paleozoic. The processed data was rotated by 45 degrees using a window designed over the dominant Mesozoic reflections (Peter Cary, personal communication). A more detailed sample-by-sample rotation may be required to detect any depth variance in the natural polarization axis. The delay time maps introduce a new complexity to how a stress field manifests itself locally within the sedimentary column. A direct application of local stress mapping is in reservoir modelling and development.

The Vp/Vs values mapped in the Viking for both S1 and S2 (between 1.7 and 2.6) are within the ranges for sand and shale found in core data (Miller, 1992) and a seismic example in California. (Tatham and Krug, 1985). The Vp/Vs anomaly in the

Viking could become more obvious if the sands were charged with less than 10% gas (Tatham and McCormack, 1991).

The ratio calculation in equation 1 weights the Vp/Vs calculation toward changes in the Vs interval which is the lower bandwidth volume and generally the more difficult data volume to interpret. Therefore, the Vp/Vs values are more sensitive to errors to the picks in the shear section. Calculations of Vp/Vs on 2-D stacked sections assume an isotropic medium, which is not the case. 3-D removes this ambiguity and values can be mapped based upon the polarization of the shear-wave.

The data quality of the S1 and S2 volumes should be more comparable. The differences between S1 and S2 can be attributed to a more detailed effort in the velocity analysis on the S1 (Peter Cary, personal communication).

The Vp/Vs ratio map for S1 and S2 in the carbonate section are puzzling in that the Vp/Vs values within the 1 square mile patch are higher than the expected value for dolomite (1.8). A possible explanation for this discrepancy is that there is more than one variable in the interval that is changing. Porosity, not lithology, may be the dominant influence on the mapped Vp/Vs ratio within the Nisku. The Vp/Vs ratio is sensitive to two opposing variables in this interval. From well data, there is an increasing porosity and a lithologic change from anhydrite to dolomite east of the analyzed patch. The sensitivity of the Vp/Vs ratio toward these two variables are in the opposite direction, and Robertson (1987) has found a measured increase in Vp/Vs of dolomite as the pore shape became more linear. The interval may be filled with variations of dolomite and anhydrite along with changes in the pore geometry. The latter influences can increase the Vp/Vs ratio above 1.8. These factors may override the influence of lithology change within the carbonate interval.

Because the wide intervals (over 200ms), the calculated ratios are not as sensitive to variations solely within the Nisku. The Nisku makes up only 15% of the total interval and variations within it may be masked by the background of Wabamun and Calmar formations. Also, below the Mannville coal, the reduced resolution lowers the confidence of the horizon picks, adding more error to the measurement. The reduced resolution in the S1 and S2 prevented smaller correlatable horizons from being used.

The wealth of data that a 3-D survey presents allow the interpretation of patterns elastic properties in plan view. The S1-S2 delay maps show that neither Vs1 nor Vs2 is constant throughout and interval because of local variations in the stress field. The patterns can be biased by survey acquisition, and it is the responsibility of the interpreter in dealing with these sophisticated data sets to be aware of the possible acquisition and processing assumptions that can bias the data.

In a historical context, P-S 3-D is now developing much like conventional 3-D was only a decade ago. As the economic aspects of our industry become more dominant, we must provide more quantifiable criteria to our economic models. Converted-wave data can help add a more quantitative value to risk. Multicomponent seismic techniques, like conventional 3-D, will become an essential tool in exploration risk reduction and investment optimization.

CONCLUSIONS

Multicomponent converted-wave 3-D data provides additional elastic wave information to conventional P-wave data. This allows the construction of a more integrated interpretation that includes acoustic and elastic information in three dimensions.

Common conversion point (CCP) fold maps must be included as a criteria in future multicomponent 3-D acquisition designs. The CCP fold in the Joffre survey compromised the converted-shear amplitudes.

The P-S1 and P-S2 data volumes are of excellent data quality and have imaged all reflectors to the Precambrian basement. This has allowed the correlation of key horizons between the acoustic and the converted-wave data volumes in the construction of Vp/Vs maps.

Vp/Vs mapping of dolomite within the Nisku is not as expected because of a wide interval of calculation, the 2000m depth of the target, and the presence of anhydrite within the interval.

Lateral variations in Vp/Vs have been mapped in the Viking formation which can be attributed to lateral sand presence. Lateral variations in the stress field have been mapped using delay-time measurements between S1 and S2.

Lateral Vp/Vs estimates from correlations of P, S1, and S2 volumes provide a powerful lithologic information not otherwise found in a conventional P-wave section.

FUTURE WORK

The prestack data must be revisited in smaller time gates to evaluate the robustness of a 45 degree rotation for the entire data set. P-SV and P-P AVO analysis also needs to be applied and investigated to help determine lithology changes in the Nisku and fractures within the Second White Speckled Shale.

ACKNOWLEDGMENTS

REFERENCES

Al-Bastaki, A.R., Arestad, J.F., Bard, K., Mattocks, B., Rolla, M.R., Sarmiento, V., Windells, R., 1994, Progress report on the characterization of Nisku carbonate reservoirs: Joffre field, south-central Alberta, Canada, *in:* Reservoir characterization project - phase 5 report, Colorado School of Mines.

Anderson, J.H. and Machel H.G., 1987, Deposition and diagenetic evolution of the Upper Devonian Nisku reef trend of Central Alberta, *in:* Canadian Reef Inventory Project, Reef Research Symposium, Banff, Alberta, Can. Soc. Petrol. Geol. Abstracts, 16.

Anderson, N.L., White, D. Hinds, R., 1989, Woodbend group. in: Geophysical Atlas of Western Canadian Hydrocarbon Pools, Anderson, N.L., Hills, L.V., and Cederwall, D.A., eds.: Canadian Society of Exploration Geophysicists/Canadian Society of Petroleum Geologists Joint Publication.

Babcock, E.A., 1978, Measurement of subsurface fractures from dipmeters: AAPG Bulletin, **62**, 7, 1111-1126.

Buchanan R., 1992, Three-dimensional seismic: The application of new technology to oil field development: Bull. Amer. Assoc. Petrol. Geol., **76**, 1855-56.

Cary, P.W., 1994, 3D converted-wave processing, Joffre survey, *in*: 3D-3C seismic exploration, CREWES Project tutorial notes.

Chevron Exploration Staff, 1979, The geology, geophysics, and significance of the Nisku reef discoveries, West Pembina area, Alberta, Canada: Bull. Can. Petrol. Geol., **27**, 326-359.

Colorado School of Mines, 1994, Reservoir characterization project phase 4 report, Colorado School of Mines.

Davis, T.L., Schuck, E.L., and Benson, R.D., 1993, Coalbed Methane Multicomponent 3D Reservoir Characterization Study, Cedar Hills Field, San Juan Basin, New Mexico: 63rd Ann. Internat. Mtg. Soc. Expl. Geophys., Expanded Abstracts, 275-276.

Eaton, D.W.S., and Lawton, D.C., 1992, P-SV stacking charts and binning periodicity: Geophysics, **57**, 745-748.

Energy Resources Conservation Board, 1992, Alberta's reserves of crude oil, oil sands, gas, natural gas liquids, and sulfur: ERCB Publication.

Garotta, R., Marechal, P., and Magesan, M., 1985, Two component acquisition as a routine procedure for recording P-waves and converted waves: Jour. Can. Soc. Explor. Geophys., **20**, 440-54.

Gilhooly, M.G., 1986, Sedimentology and geologic history of the Upper Devonian (Frasnian) Nisku and Ireton Formations, Bashaw area, Alberta. Unpublished MSc. thesis, The University of Calgary.

Goodaway, W.N. and Mayo, L.F., 1994, Multicomponent seismic and borehole experiment to establish and identify the cause of anisotropy in the 2nd white specks at Garrington, Alberta: 64th Ann. Internat. Mtg. Soc. Expl. Geophys., Expanded Abstracts, 248-251.

Harrison, M.P., 1992, Processing of P-SV surface-seismic data: anisotropy analysis, dip moveout, and migration: Unpublished PhD. dissertation, The University of Calgary.

Lane, M.C., and Lawton, D.C., 1993, 3-D converted-wave asymptotic binning: CREWES Research Report, **5**, 29-1 - 29-5.

Lawton, D.C., 1993, Optimum bin size for converted-wave 3-D asymptotic mapping: CREWES Research Report, **5**, 28-1 -28-14.

Leckie, D.A., Bhattacharya, J.P., Bloch, J., Gilboy, C.F., Norris, B, 1994, Cretaceous Colorado/Alberta group. In: Geological Atlas of the Western Canada Sedimentary Basin. G.D. Mossop and I. Shetson (comps.). Calgary, Canadian Society of Petroleum Geologists and Alberta Research Council, chpt. 20.

Machel, H.G., 1983, Facies and diagenesis of some Nisku buildups and associated strata, Upper Devonian, Alberta, Canada, in: Carbonate buildups - A core workshop, Soc. Econ. Paleo. and Min., Workshop No.4, Harris, P.M., ed., 114-181.

Miller, S.L.M., Well log analysis of Vp and Vs in carbonates: CREWES Research Report, **4**, 12-1 - 12-11.

Mueller, M.C., 1991, Prediction of lateral variability in fracture intensity using multicomponent shear-wave surface seismic as a precursor to horizontal drilling in the Austin Chalk: Geophys. J. Int. 107, 409-415.

Oosterbaan, J.M., 1990, 3-D seismic as an exploration tool: 60th Ann. Mtg. Soc. Expl. Geophys., Expanded Abstracts, 160-161.

Reinson, G.E., Warters, W.J., Cox, J., Price, P.R, 1994. Cretaceous Viking formation, *in:* Geological Atlas of the Western Canada Sedimentary Basin. G.D. Mossop and I. Shetson (comps.). Calgary, Canadian Society of Petroleum Geologists and Alberta Research Council, chpt. 21.

Rennie, W, Leyland, W, and Skuce, A., 1989., Winterburn (Nisku) Reservoirs, *in* : Geophysical Atlas of Western Canadian Hydrocarbon Pools, Anderson, N.L., Hills, L.V., and Cederwall, D.A., eds.: Canadian Society of Exploration Geophysicists/Canadian Society of Petroleum Geologists Joint Publication.

Robertson, J.D., 1987, Carbonate porosity from S/P traveltime ratios: Geophysics, **52**, 1346-1354.

Robertson, J.D., 1992, Reservoir management using 3-D data, *in:* Reservoir Geophysics: Sheriff, R.E., ed., Society of Exploration Geophysics.

Stewart, R.R., Pye, G., Cary, P.W., and Miller, S.L.M., 1993, Interpretation of P-SV seismic data: Willesden Green, Alberta: CREWES Research Report, **5**, 15-1 - 15-19.

Stokes, F.A., 1987, Evolution to the upper Devonian of Western Canada, *in:* Principles and concepts for exploration and exploitation of reefs in the Western Canada basin, Boy, G.R., and Hopkins, J.C., eds., Can. Soc. Petrol. Geol. Short Course Notes, 1-36.

Switzer, S.B., Holland, W.G., Christie, D.S., Graf, G.C., Hedinger, A.S., McAuley, R.J., Wierzbicki, R.A., and Packard, J.J, 1994 Devonian Woodbend-Winterburn strata of the western Canada sedimentary basin *in:* Geological Atlas of the Western Canada Sedimentary Basin. G.D. Mossop and I. Shetson (comps.). Calgary, Canadian Society of Petroleum Geologists and Alberta Research Council, chpt. 12.

Tatham, R.H. and Krug, E.H., 1985, Vp/Vs interpretation, *in:* A.A. Fitch, Ed., Developments in geophysics-6: Elsevier Appl. Sci. Publ, 139-188.

Tatham, R.H. and McCormack, M.D., 1991, Multicomponent seismology in petroleum exploration: Investigations in geophysics - 6, Society of Exploration Geophysicists.

Tatham, R.H., and Stewart, R.R., 1993, Present status and future directions of shear-wave seismology in exploration: CREWES Research Report, **5**, 1-1 - 1-21.

Watts, N.R., 1987, Carbonate sedimentology and depositional history of the Nisku Formations within the Western Canadian Sedimentary Basin) in south central Alberta, *in:* Devonian lithofacies and reservoir styles in Alberta, Krause, F.F., and Burrowes. O.G., eds., 87-152.

Yardley, G.S., Graham, G., and Crampin, S., 1991, Viability of shear-wave amplitude versus offset studies in anisotropic media: Geophys. J. Int., **105**, 493-503.

Table 1 - 3-D - 3C Survey Design Parameters:

Survey Size: 3240m (N-S) x 4200 m (E-W)
Source Points: 742
Receiver Stations: 810
Receiver Lines: 15
Total Bins: 15 650
Bin Size: 30m x 30m
Number of Patches: 4
Fold
       Maximum: 44
       Average: 15

Patch Details
Number of Patches: 4
Size: 3240m (N-S) x 1500m (E-W)
Receiver Lines (N-S)
       Number: 6
       Line Spacing: 300m
       Receivers/Line: 54
       Receiver Spacing: 60m
Source Points/Patch: 159 to 212
Source Lines (E-W)
       Line Spacing: 60m
       Source Spacing: 300m

Source Details
       1 Vibrator/Source Point
       Sweep Length: 12 Seconds - Linear
       Frequency Range: 10-120 Hz - Up Sweep
       Number of Sweeps : 7
       Listen Time: 4 Seconds

Geophones
       3 Component
       OYO SHC-3-D 10Hz. natural frequency

Instrumentation
       I/O System 2
       Sample Rate: 2ms

(Modified from Colorado School of Mines, 1992)

				WINTERBURN BASIN		NISKU SHELF	
				WINDFALL-OBED, ALTA	PEMBINA, ALTA	LEDUC-DRUMHELLER, ALTA	SASKATCHEWAN
U P P E R D E V O N I A N	F R A S N I A N	F A M E N N I A N / W A B A M U N	W A B A M U N GP	WABAMUN GP	WABAMUN GP	WABAMUN GP	THREE FORKS FM
		W I N T E R B U R N G P		"GRAMINIA SILT" / BLUERIDGE MBR / WINTERBURN CARBONATE / "NISKU REEF" CALMAR FM	"GRAMINIA SILT" / BLUERIDGE MBR / CALMAR FM	CALMAR FM	
				"WINTERBURN SHALE"	WOLF LAKE MBR / CYNTHIA MBR / ZETA LAKE MBR / BIGORAY MBR / LOBSTICK MBR	"UPPER NISKU" / "LOWER NISKU" — N I S K U F M	"UPPER BIRDBEAR" / "LOWER BIRDBEAR" — B I R D B E A R F M
		W O O D B E N D G P	LEDUC FM / "PEECHEE" / "CAIRN"	IRETON FM	IRETON FM	CAMROSE MBR / IRETON FM / LEDUC FM	DUPEROW FM
					DUVERNAY FM	DUVERNAY FM	
					MAJEAU LAKE FM	COOKING LAKE FM	
		BHL GP	BEAVERHILL LAKE GP	BEAVERHILL LAKE GP	BEAVERHILL LAKE GP	SOURIS RIVER FM

Figure 1: Stratigraphic nomenclature for the Upper Devonian in the central Alberta Basin. Joffre resides in the Nisku Shelf (Leduc-Drumheller). From Rennie et al, 1989.
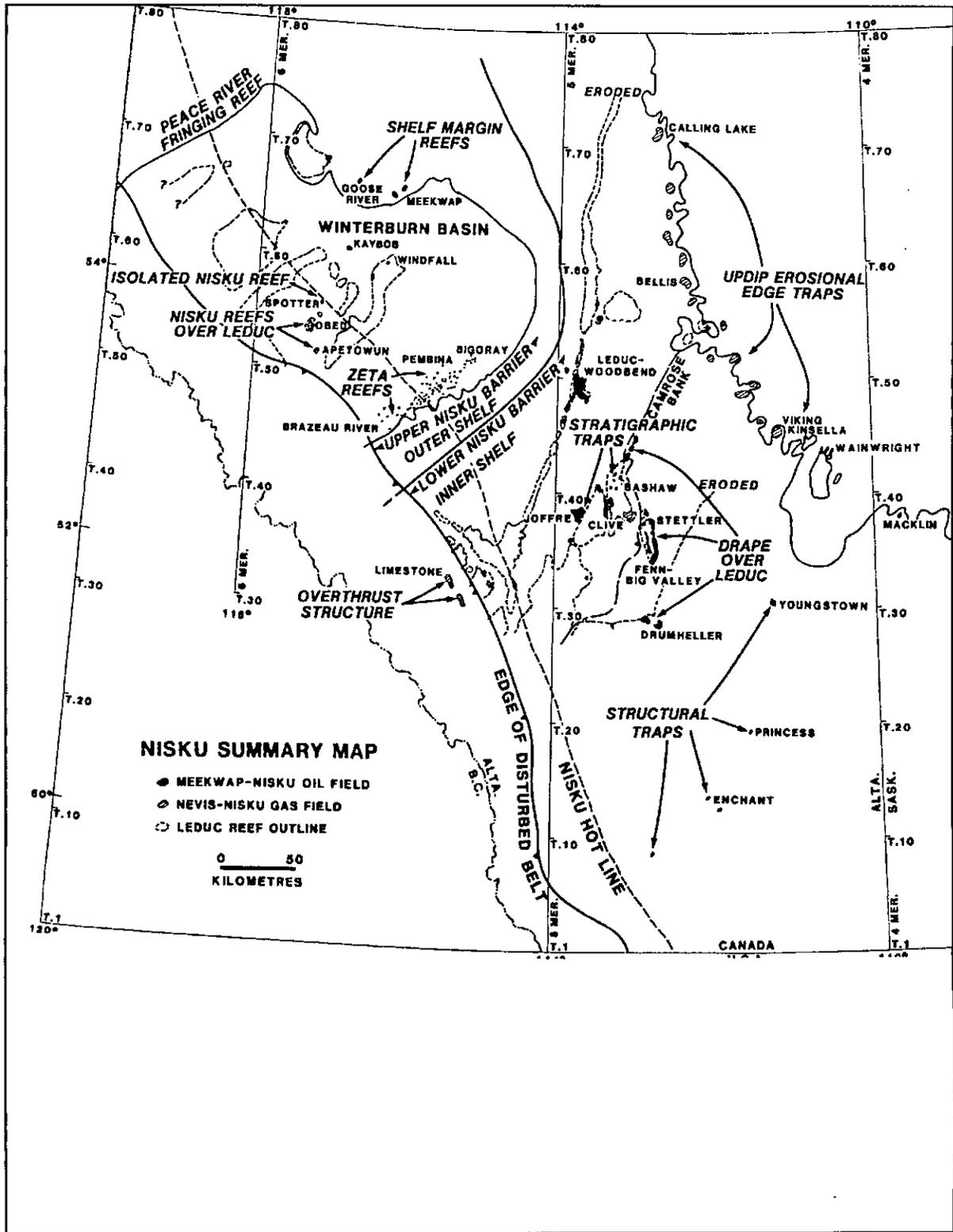
Figure 2: Nisku Field Summary Map for the Western Canadian Sedimentary Basin. The Joffre field is located near Twp. 40 and Rge. 5W6. From Rennie et al., 1989.

Rge. 26W4M

Twp. 39
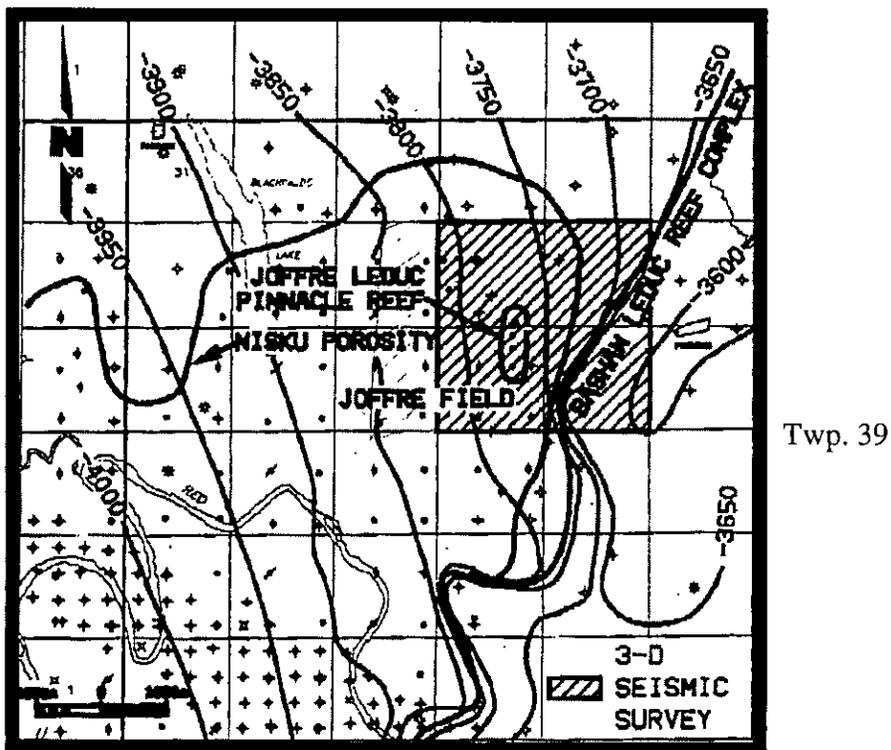
Figure 3: Geologic structure map of the Nisku formation in the Joffre area. The field is defined by the limit of porosity in the Nisku formation. Anhydrite provides the up dip and lateral seals.
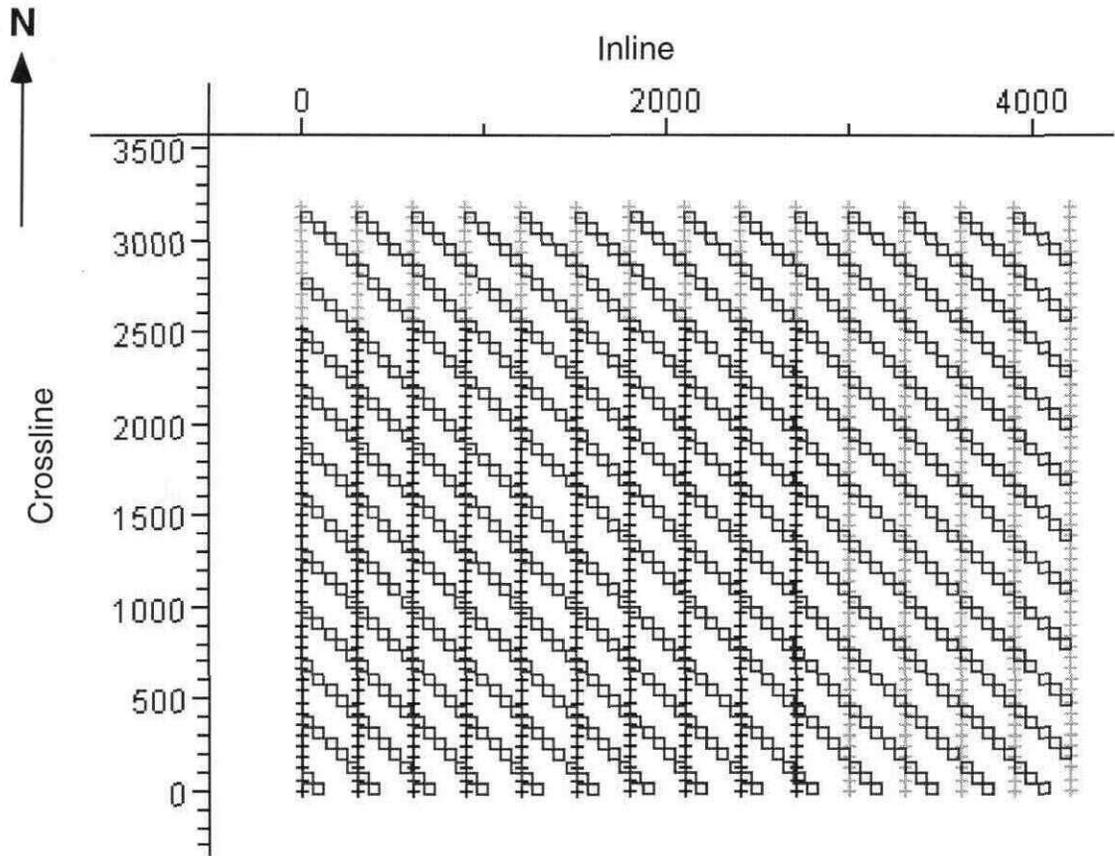
Figure 4:. Survey grid of the Joffre multicomponent survey. The source lines run at a 45 degree angle to north-south receiver lines. Units are in metres.
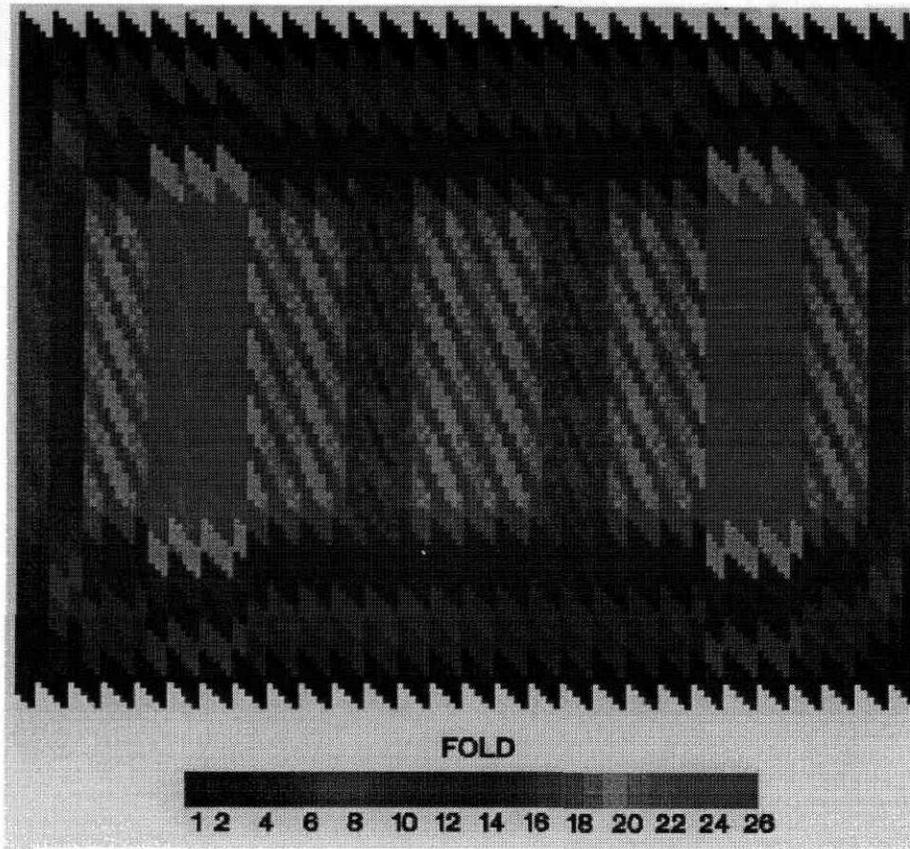
Figure 5: CMP fold of the Joffre 3-D multicomponent survey.
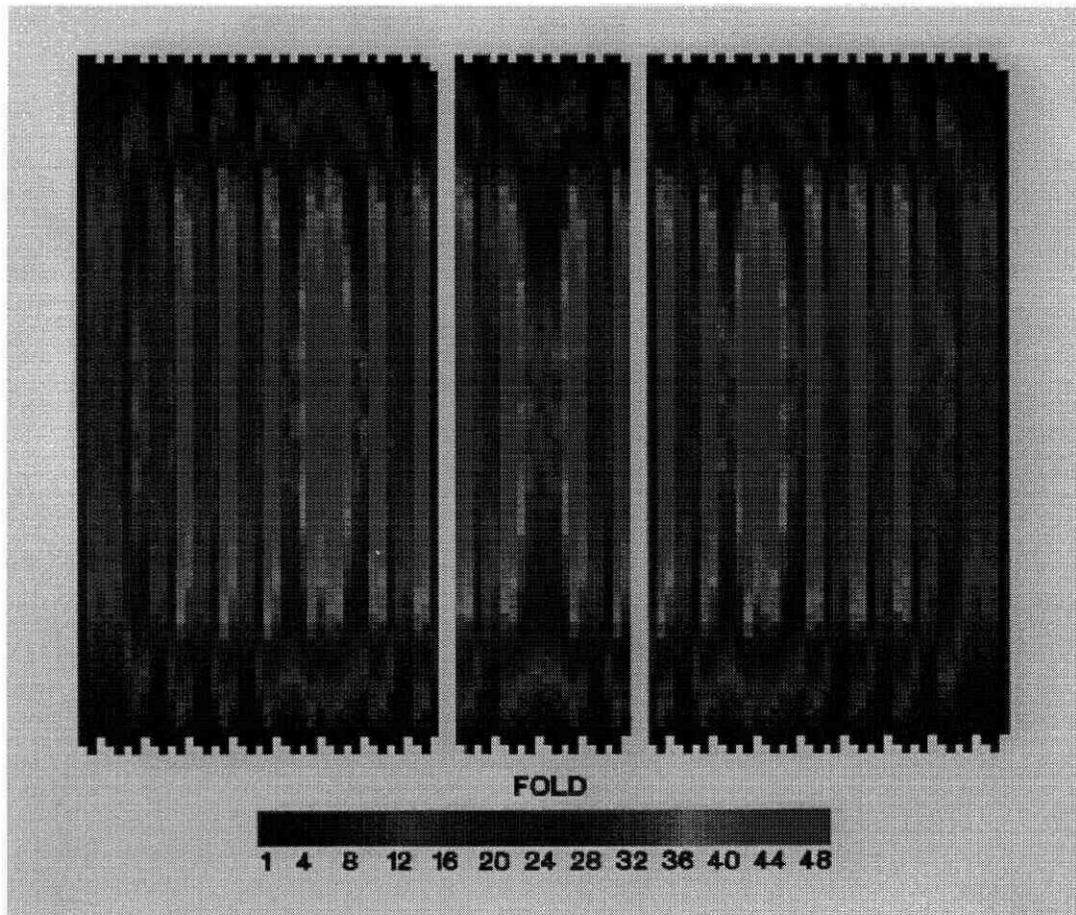
Figure 6: CCP optimized fold of the Joffre 3-D multicomponent survey. Note the fold gaps and the high periodicity of the fold in the east-west direction.

Demultiplex

↓

Geometry Assingment

↓

3D Refraction Statics

↓

Spreading Gain Correction

↓

Surface Consistent Deconvolution

↓

Brute Velocities

↓

Brute Stack

↓

Surface Consistent Statics

↓

Final Velocity Analysis

↓

Surgical Air Blast Mute

↓

Zero Phase Deconvolution

↓

Trim Statics

↓

Mute

↓

Stack

↓

Migration
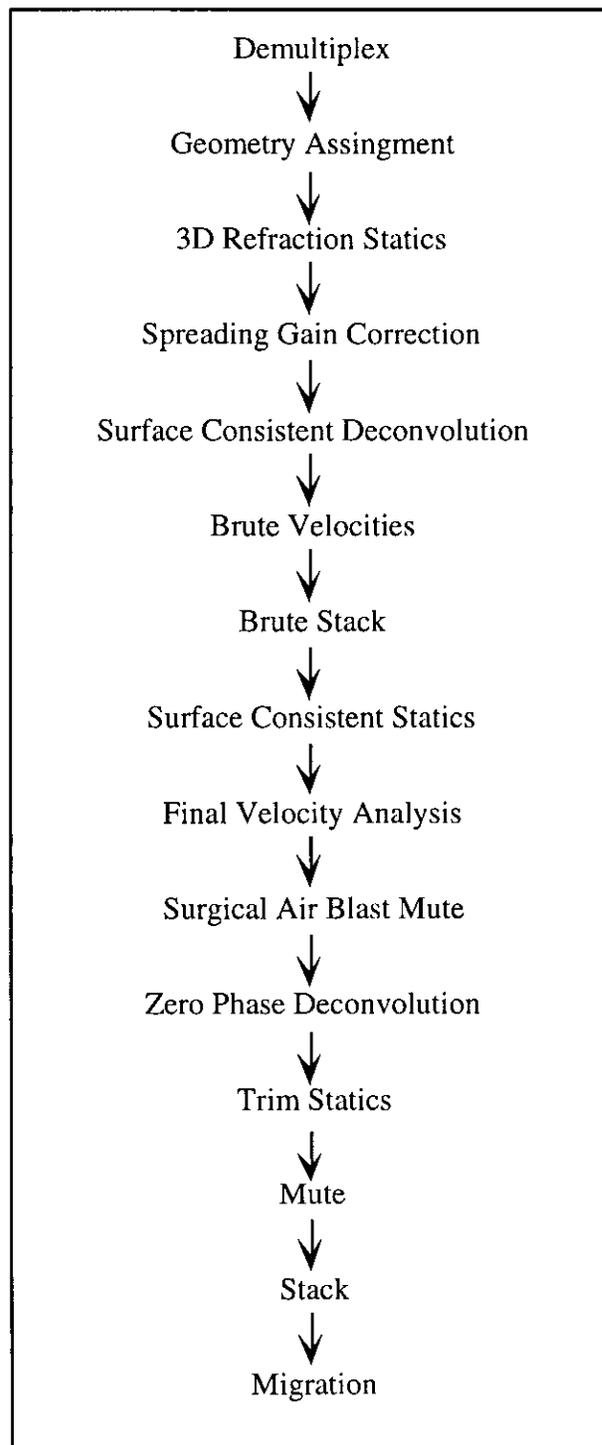
Figure 7: 3-D P-P Processing Flow. From Cary, 1994.

Process 3D P-P

↓

Rotate into (Radial, Transverse) Coordinate System
Birefringence Analysis

↓

(Harrison Rotation, Limited Azimuth Stacks)

↓

Rotate into Natural Coordinate System

↓

Geometrical Spreading Correction

↓

Surface Consistent Deconvolution

↓

Apply Source Statics (from P-P data)

↓

Brute Velocities

↓

Receiver Statics from Common-Receiver Stack

↓

P-SV Velocity Analysis

↓

Residual Surface-Consistent Statics
(using asymptotic CCP gathers)

↓

Final P-SV Velocity Analysis

↓

3-D Converted-Wave Binning
(Asymptotic - Vp/Vs = 2)

↓

3-D P-SV DMO

↓

CCP Stack

↓

Migration
(Vmig = 6 to 11% less than Vrms)

Figure 8: 3-D P-SV Processing Flow. From Cary, 1994.
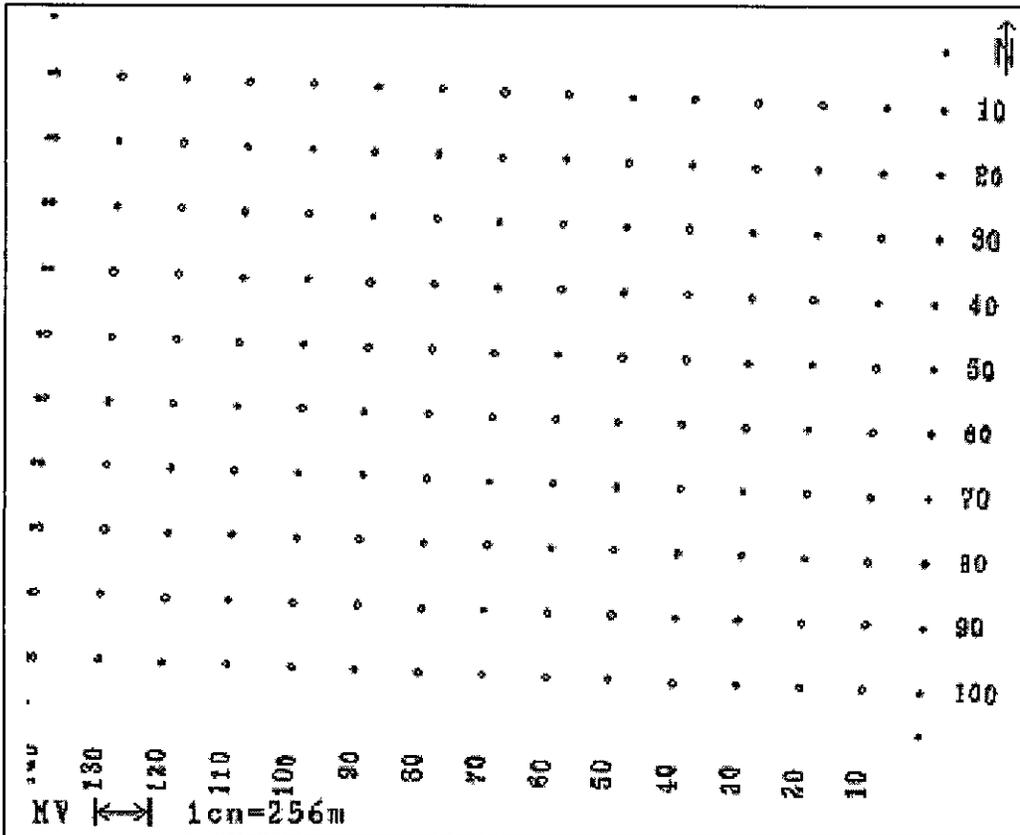
Figure 9: Geometry of the 3-D data. There are 107 crosslines (east-west direction) and 141 inlines (north-south direction).
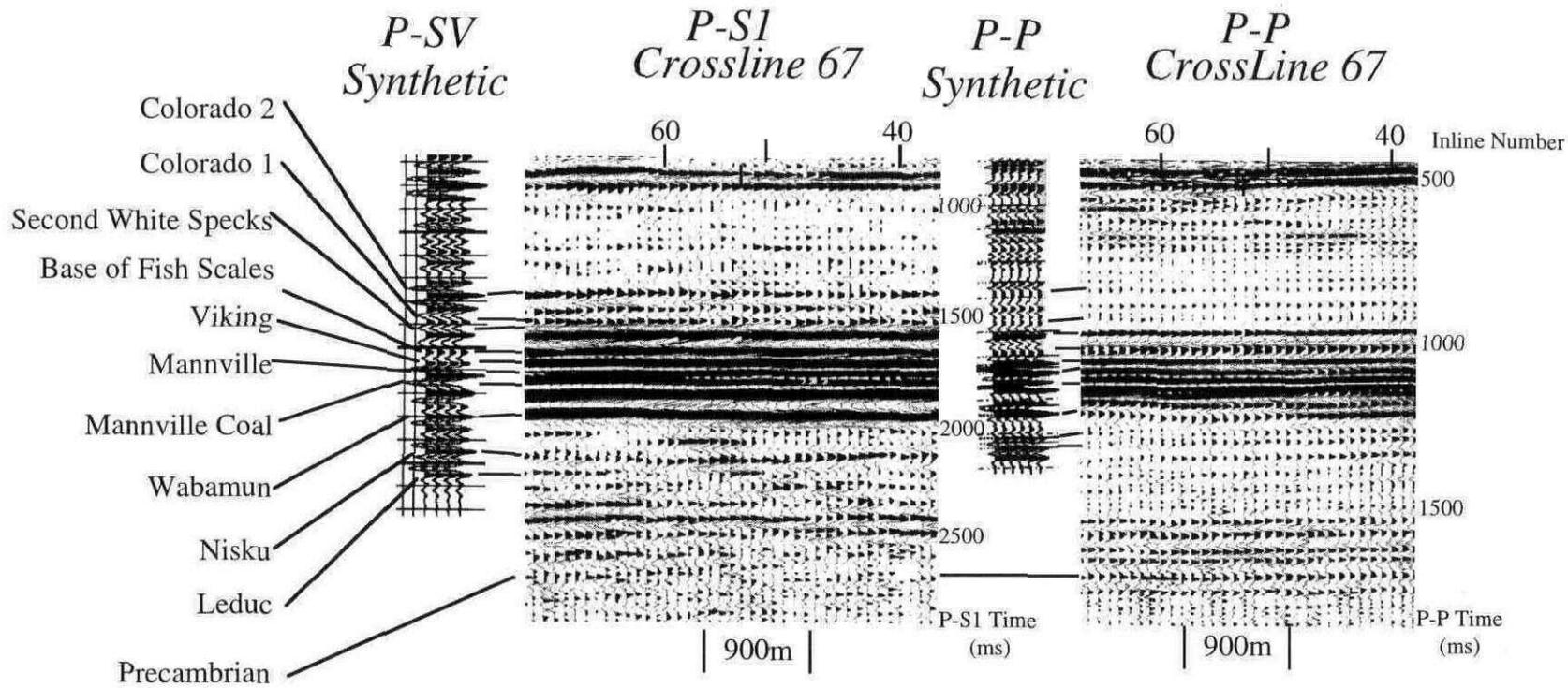
Figure 10: Event correlation of Crossline 67 between P-P and P-S1. The time scale of the P-P section has been expanded by 1.5 times to match the scale of the P-SV section.
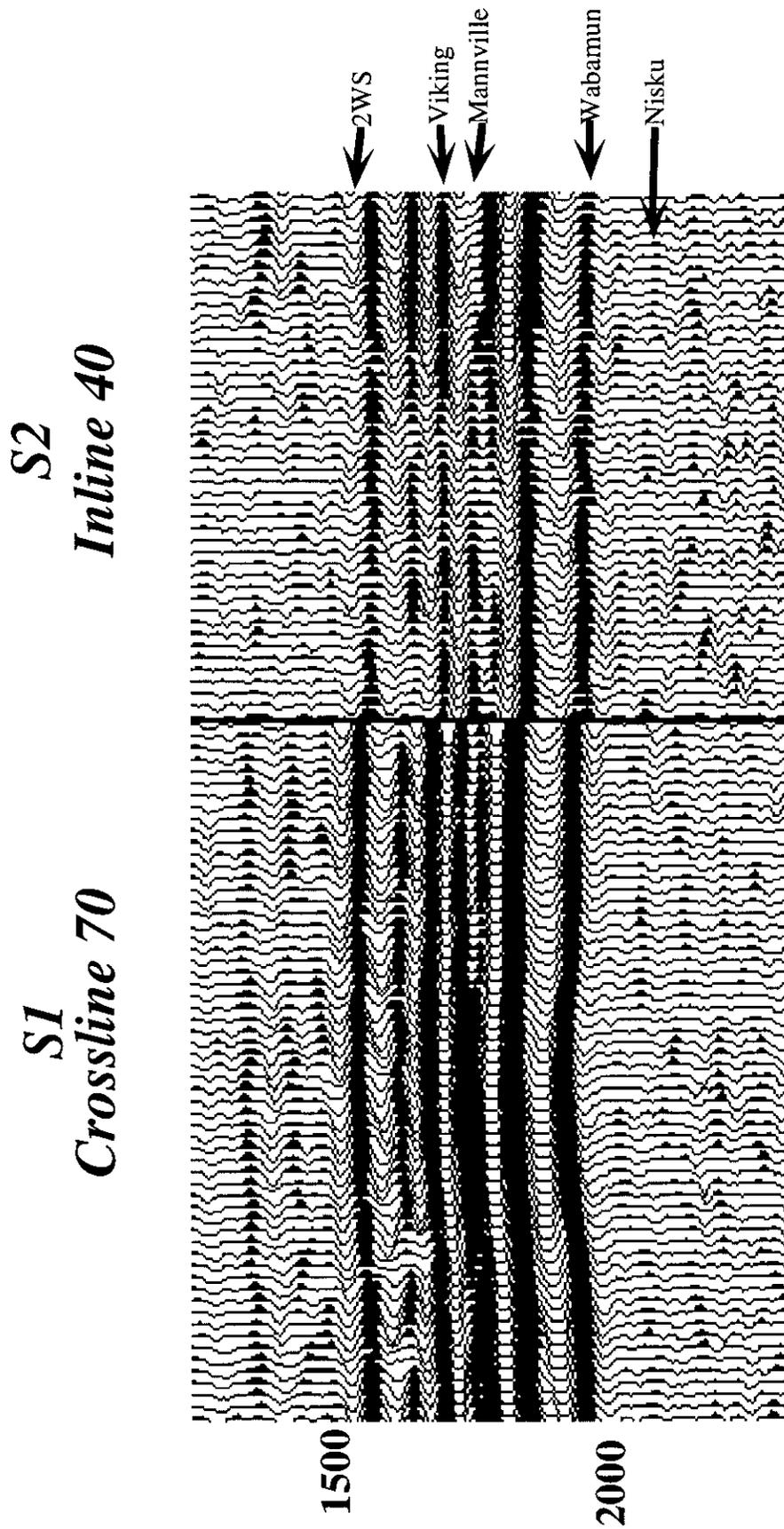
Figure 11: Tie between Crossline 70 (S1) and Inline 40 (S2).
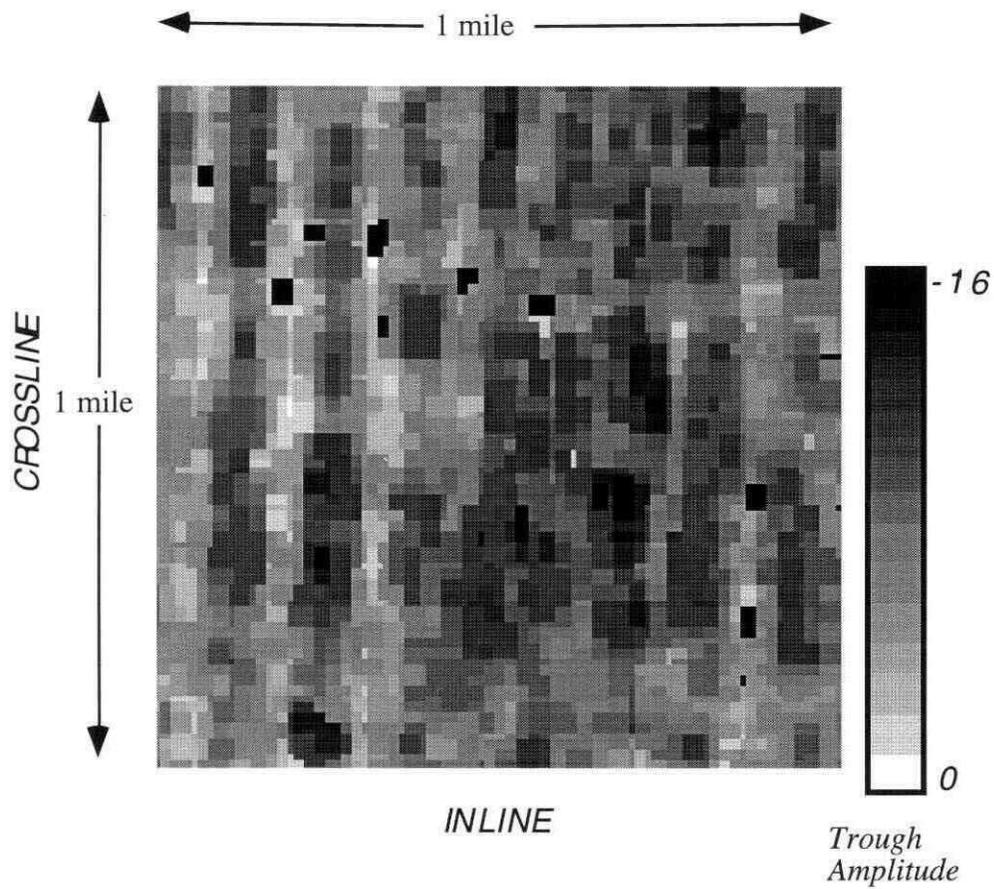
Figure 12: S1 amplitude map of the Second White Speckled Shale. The linear striped pattern follows the survey geometry.

a)

b)
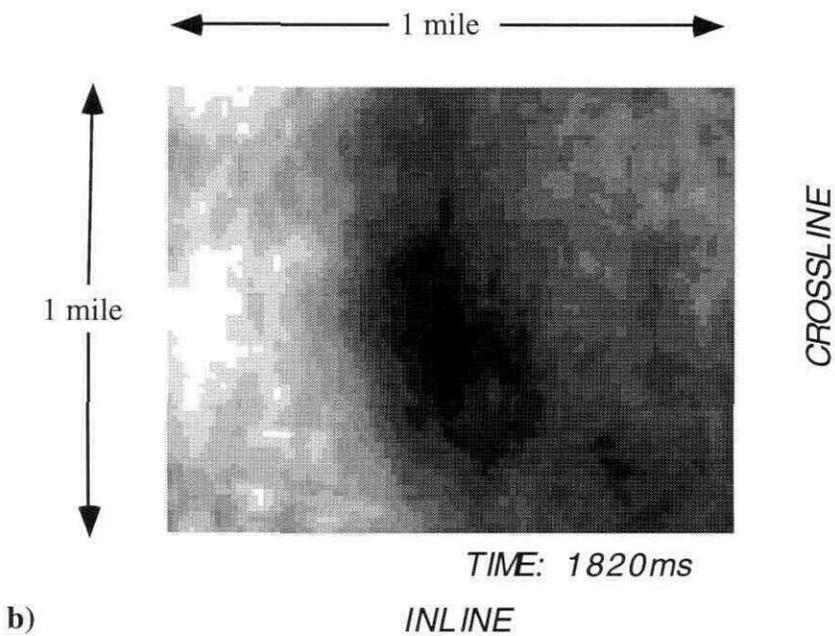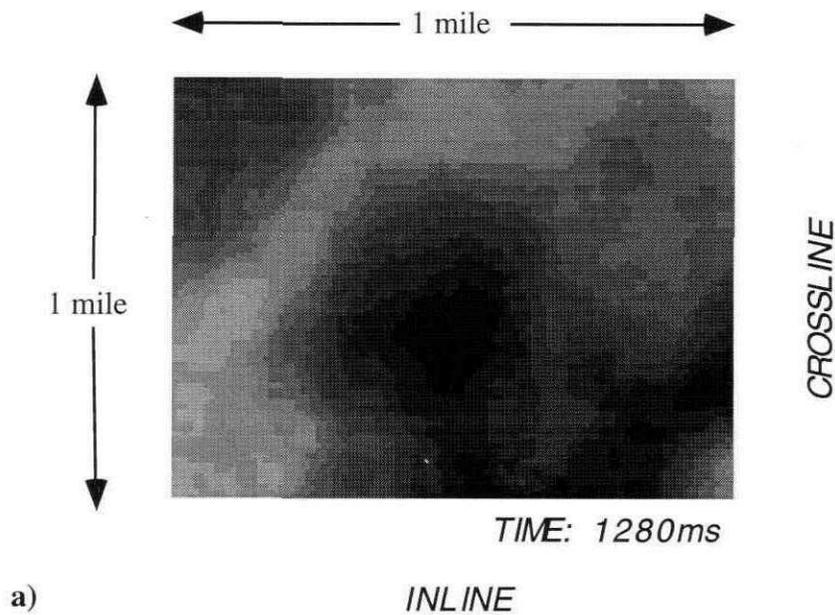
Figure 13: Time slices of P-P (upper figure) and P-SV (lower figure) at times 1280 and 1820ms, respectively. The Leduc pinnacle is located in the centre of both slices.
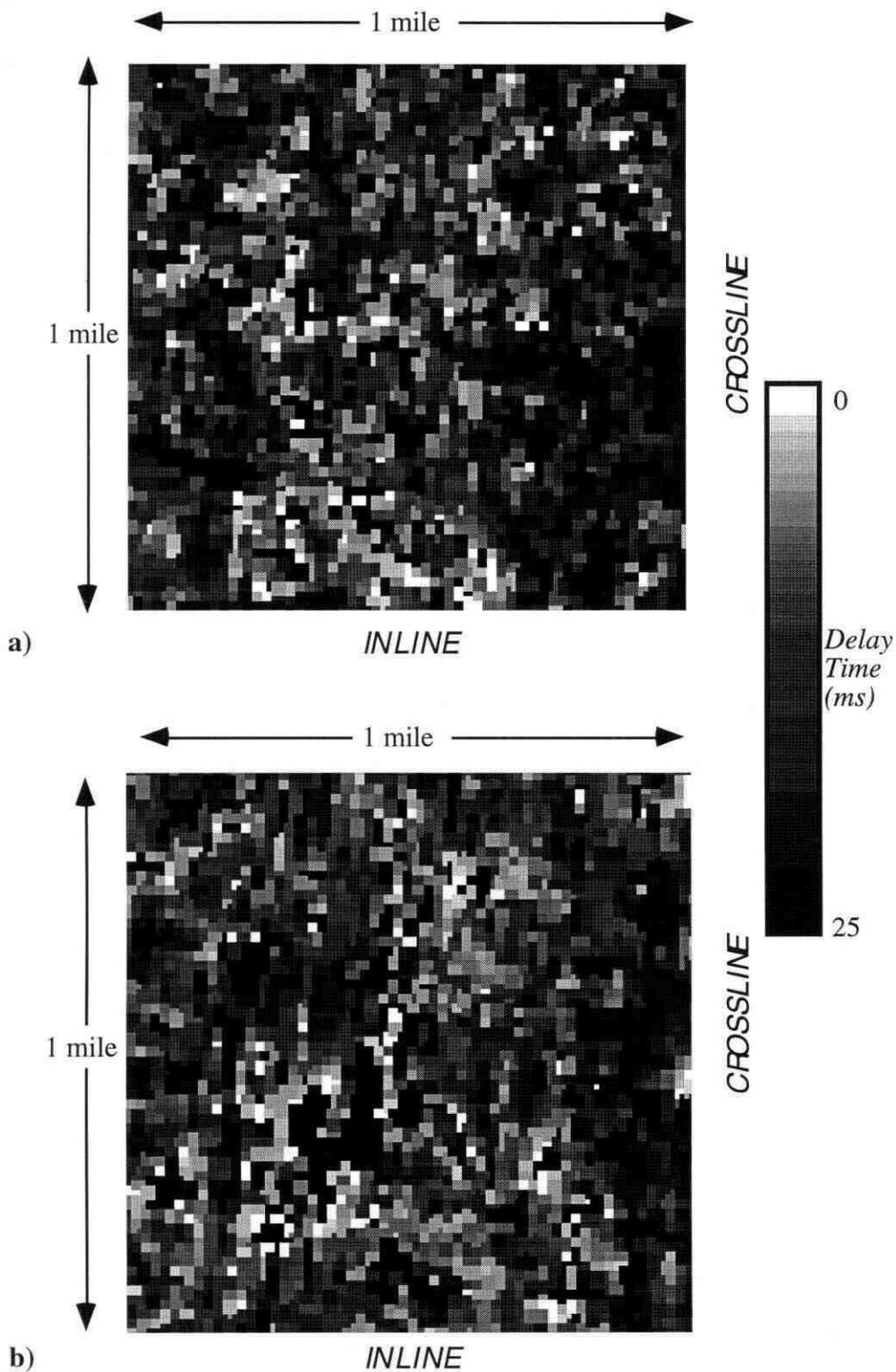
Figure 14: Time delay maps between the S1 and S2 data volumes for the Colorado event 2 (a) and the Colorado event 1 (b).
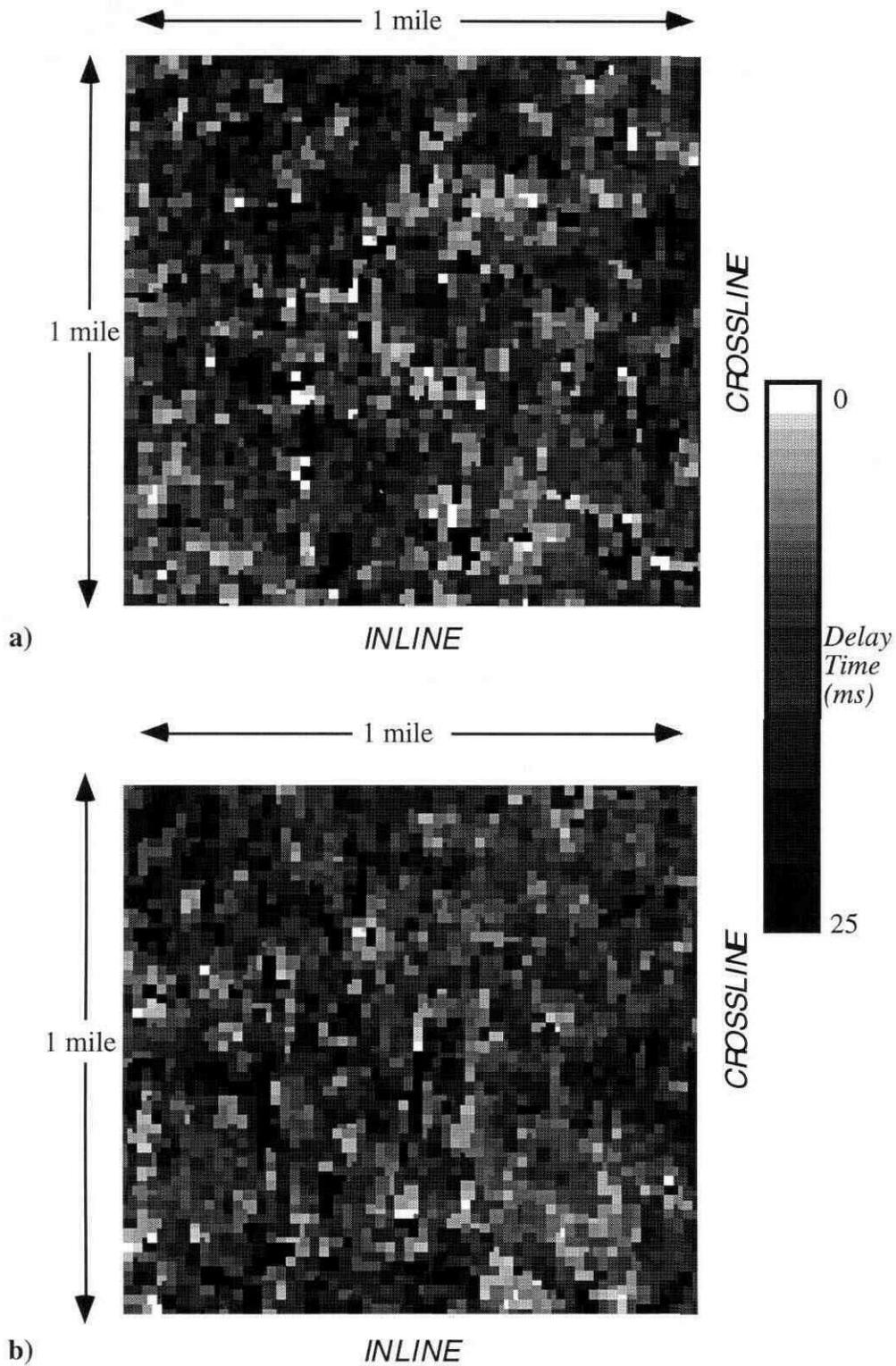
Figure 15: Time delay map between the S1 and S2 data volumes for the Second White Speckled Shale (a) and the peak one cycle below it (b).
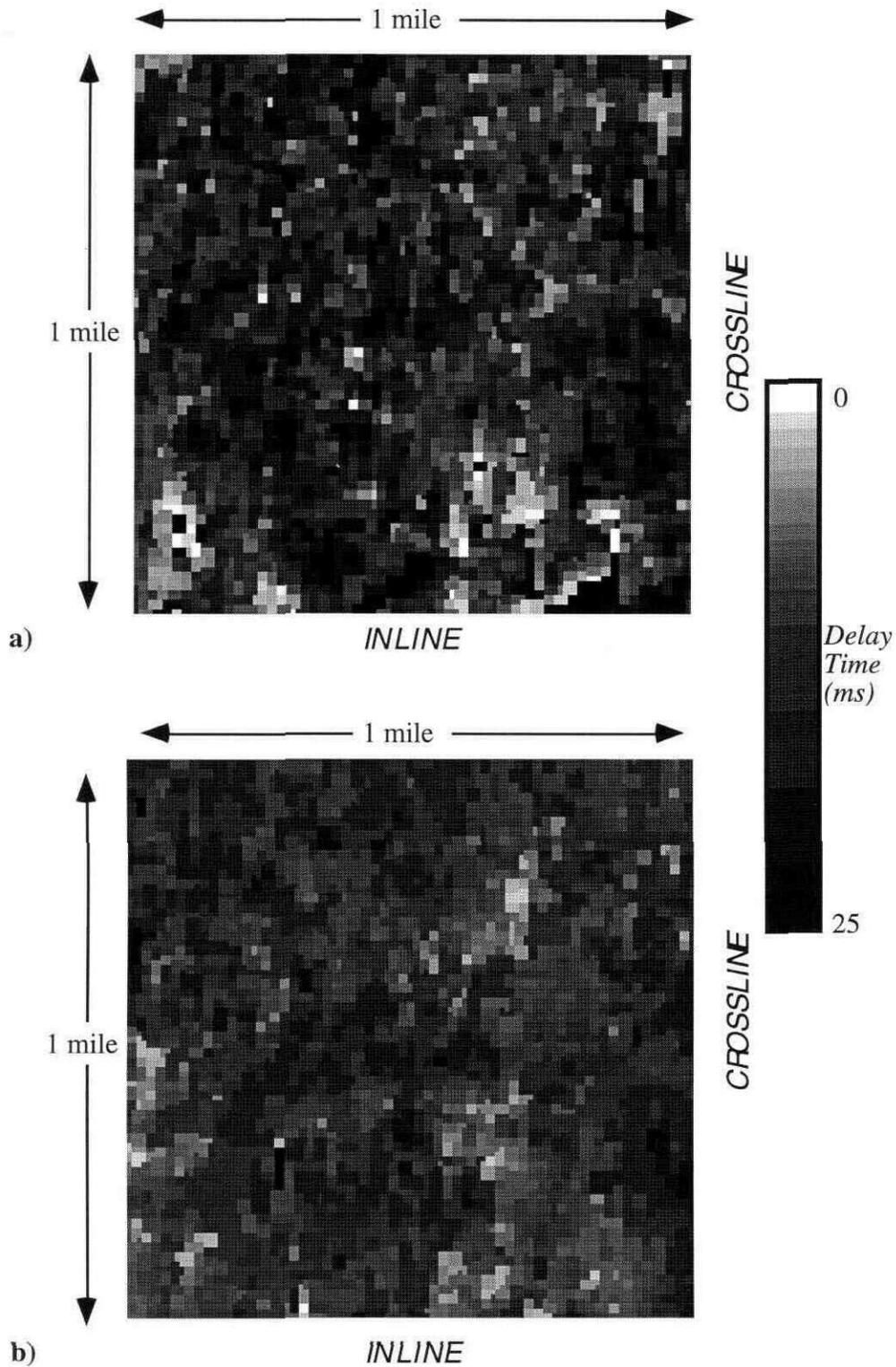
Figure 16: Time delay map between the S1 and S2 data volumes for the Base of Fish Scales (a) and the Viking (b).
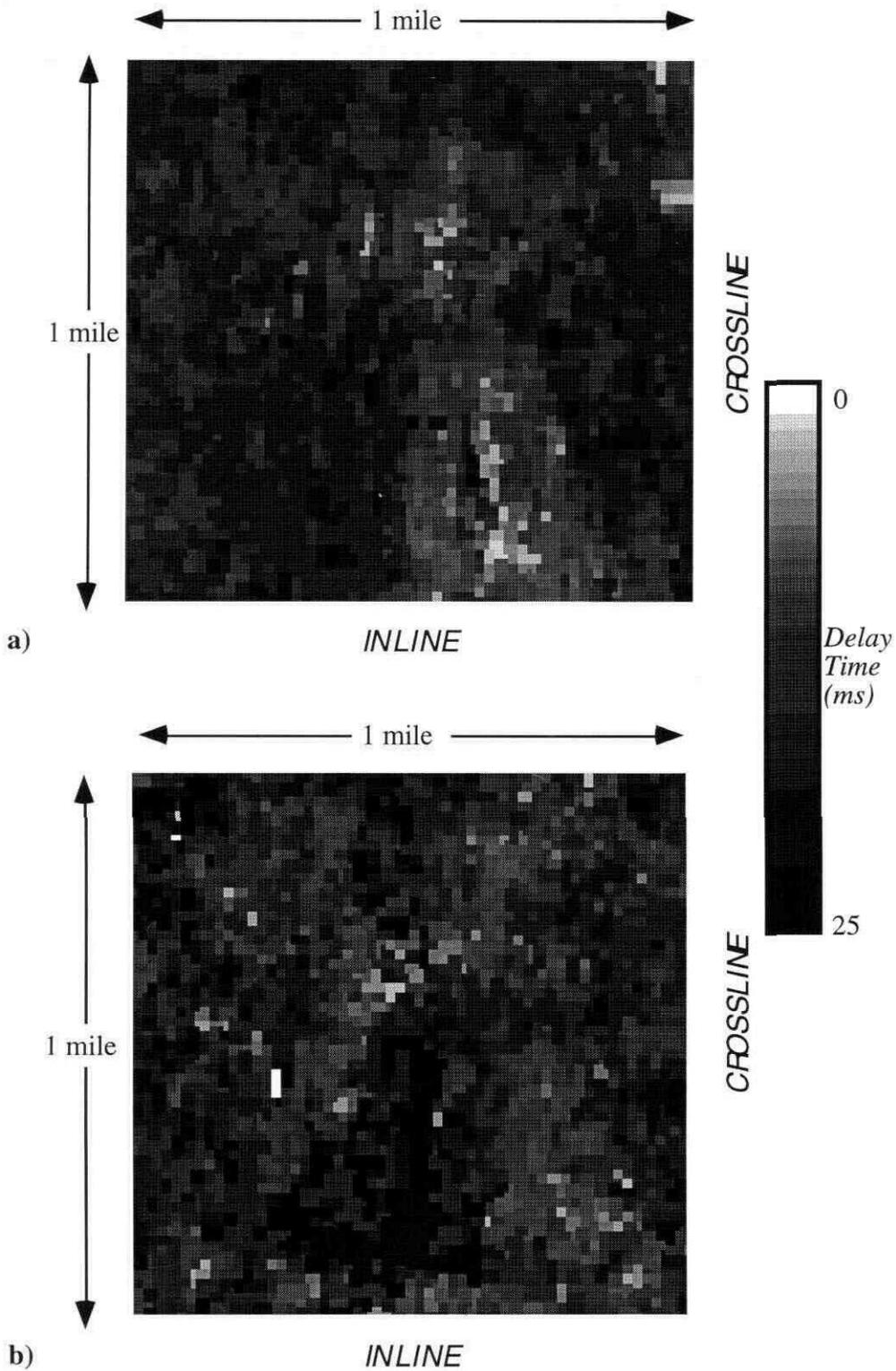
Figure 17: Time delay map between the S1 and S2 data volumes for the Mannville Coal (a) and the Wabamun (b).
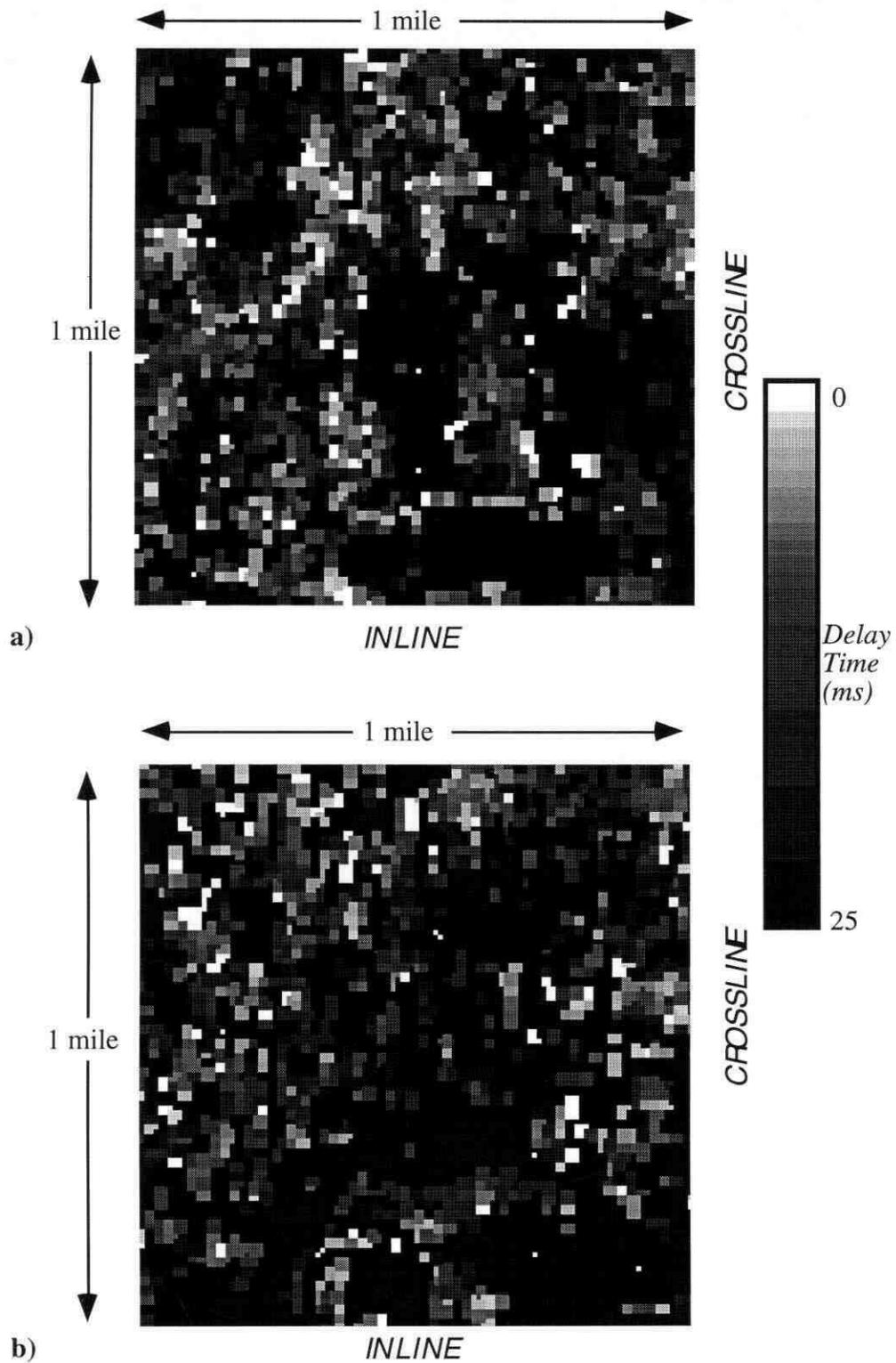
Figure 18 : Time delay maps between the S1 and S2 data volumes for the Nisku (a) and the Leduc (b).
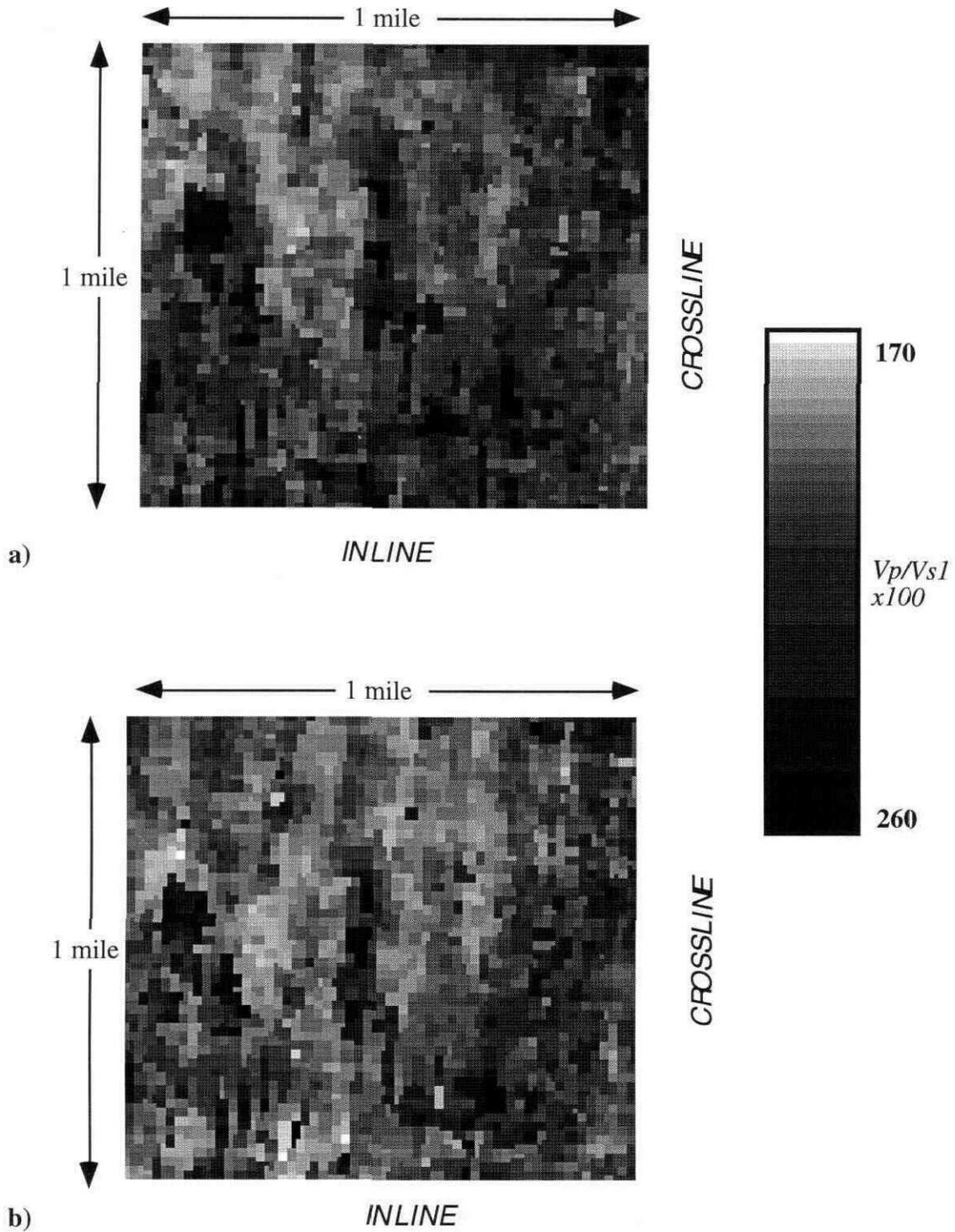
Figure 19: Vp/Vs1 ratio (x100)maps of the Viking calculated between two intervals: a) The Base of Fish Scales to the Mannville and b) Colorado event 1 and the Mannville.
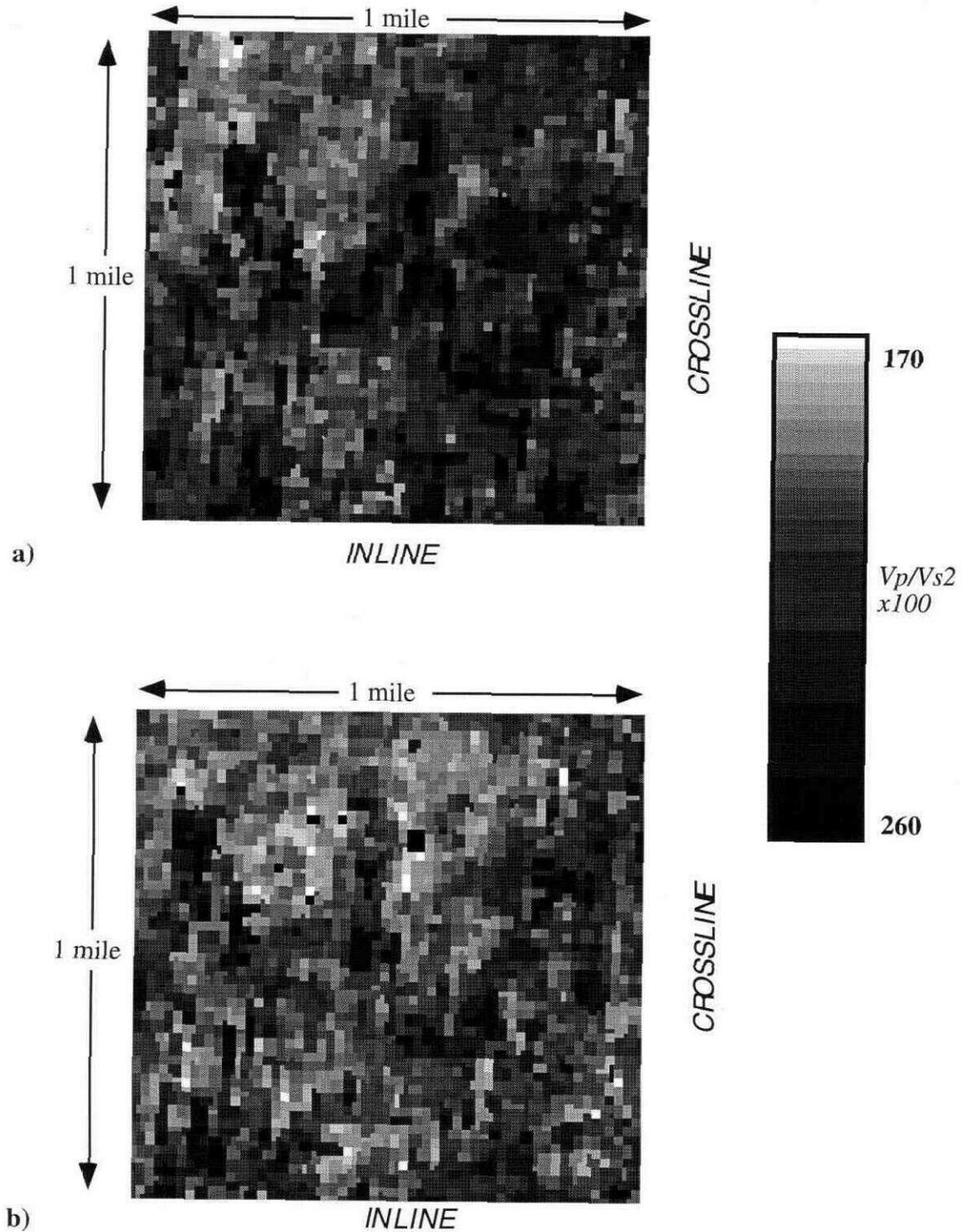
Figure 20: Vp/Vs2 ratio (x100) maps of the Viking calculated between two intervals: a) The Base of Fish Scales to the Mannville and b) Colorado event 1 and the Mannville.
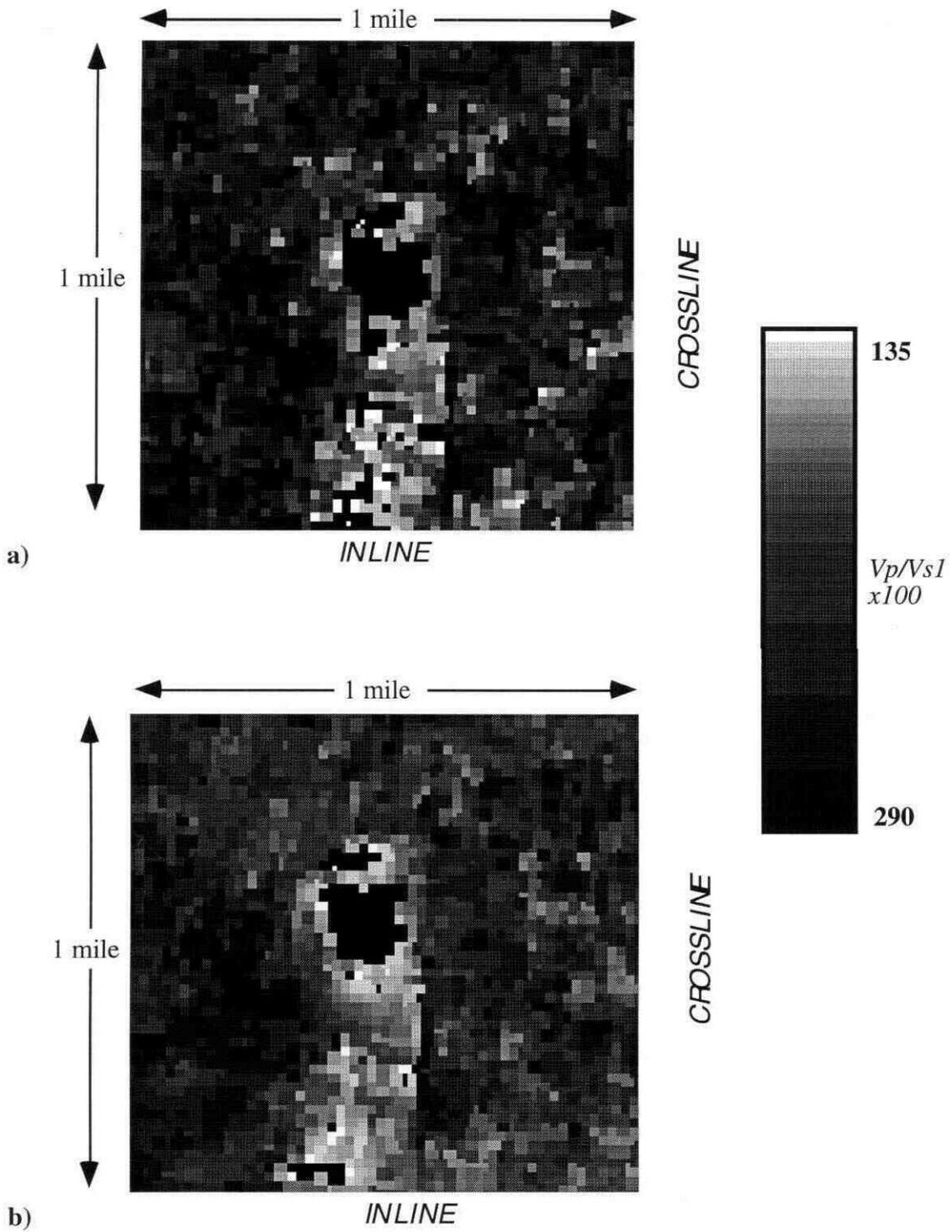
Figure 21: Vp/Vs1 ratio (x100) maps of the Nisku calculated from the Ireton to the Wabamun trough (a), and the Ireton to the Wabamun peak (b).
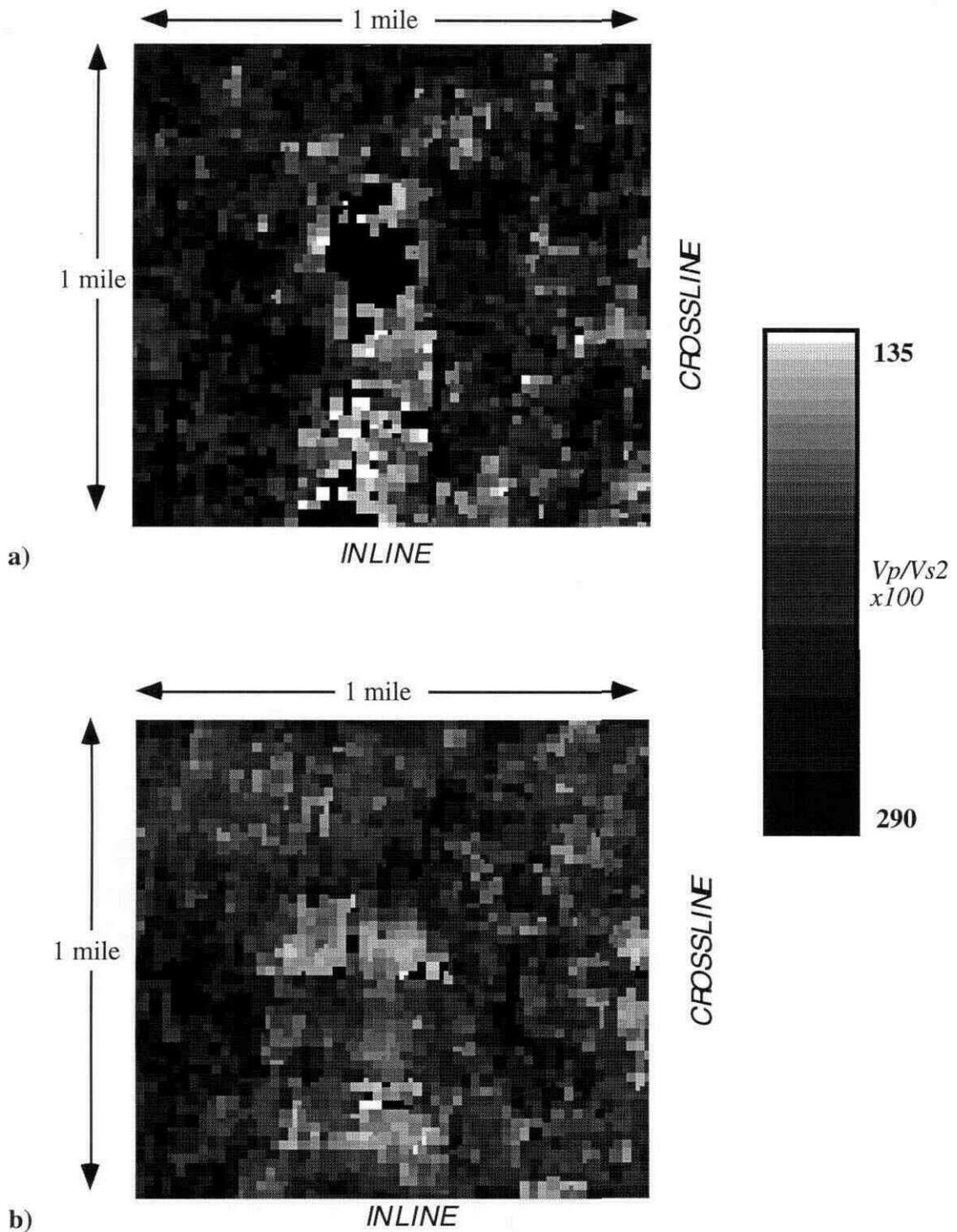
Figure 22: Vp/Vs2 ratio (x100) maps of the Nisku calculated from the Ireton to the Wabamun trough (a), and the Ireton to the Wabamun peak (b).